









Zn-Al Anticorrosive Coating Adapted to Obtain Protected Steel Wires

Marius Tintelecan¹  , Dana-Adriana Iluțiu-Varvara¹ ,
Oscar Rodriguez Alabanda² , Ioana-Monica Sas-Boca¹ ,
and Gustavo Aristides Santana Martinez³ 

¹ Technical University of Cluj Napoca, B-dul. Muncii, no. 103-105, Cluj Napoca, Romania
marius.tintelecan@ipm.utcluj.ro

² University of Córdoba, Edificio Paraninfo, Primera Planta. Campus de Rabanales, 14071
Córdoba, Spain

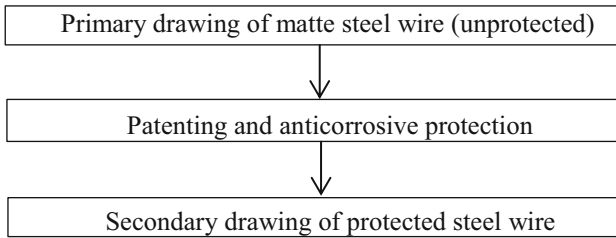
³ University of São Paulo, Engineering School of Lorena, Lorena 12602-810, Brazil

Abstract. The present work describes and quantifies the process of adding Al in thermally deposited Zn on the surface of a S235 steel wire in order to increase the anticorrosive efficiency of this protective layer. Zn crystallizes in an hexagonal system that will inevitably deform mostly by twinning. A first fundamental question is to determine which is the percentage of Al, which must be found integrated in the Zn matrix, necessary for the loss of protective layer registered when the wire is processed by drawing to the lower reduction possible. Zn-Al alloy specimens with an increasing percentage of Al have been processed by pressing. The pressing process was conducted under certain conditions of temperature and speed, simulating to a certain extent its deformation by drawing, being affected the surface of the coated steel wire. In other words, the first fundamental question of the work must be reformulated: what is the percentage of Al, which must be found in the Zn-Al alloy, in order to “forget” its deformation by twinning and to adopt its deformation by sliding? An optimal chemical composition of the Zn-Al alloy have to be determined considering that, after the deposition of “Hot Dip” on the surface of a steel wire it will be processed by drawing. It has been also analyzed the way of depositing Al in the protective layer as well as the resistance in the salt fog of the steel wires protected with this alloy. In each technical stage (subsequent deposition and drawing process) a practical comparison has been made between the variants object of this study: pure Zn (protective variant 1) and the variant: Zn-Al alloy (protective variant 2).

Keywords: Zn · Al · Deposition · Steel wiredrawing · Anticorrosiveness

1 The Technical Process

Obtaining anti-corrosion coated steel wire in any protection variant required the following steps:



The primary drawing of the matte steel wire was performed starting from a diameter of 6.0 mm to a diameter of 2.0 mm, in the dry version using partial reductions of 20%.

The patenting process was carried out in the unrolled wire, using an tunnel type oven for heating it in the austenitic field, and a sudden immersion in baths of molten Pb for sorbitization. The patenting process was made after the construction of the optimal structure (by austenitization and sorbitization) of steel wire, pickling the surface of steel wire in hydrochloric acid baths followed by fluxing the surface of the wire (in a bath containing a mixture of $ZnCl_2$ salts and NH_4Cl) and by drying its surface also in the tunnel oven. Anticorrosive protection was the technical operation by which either a layer of pure Zn (protective variant 1) or a layer of Zn-Al alloy (protective variant 2) was deposited on the surface of the steel wire. This “Hot Dip” process basically involved immersion of the wire in a bath in which the protective material is melted (so liquid) the melt having a certain temperature, and maintaining the immersion during a certain time. This experimental deposition bathtub of the Zn-Al alloy was mounted on the surface of the galvanizing bathtub itself, being partially immersed in molten zinc. The sketch of this experimental bathtub is shown in the Fig. 1:

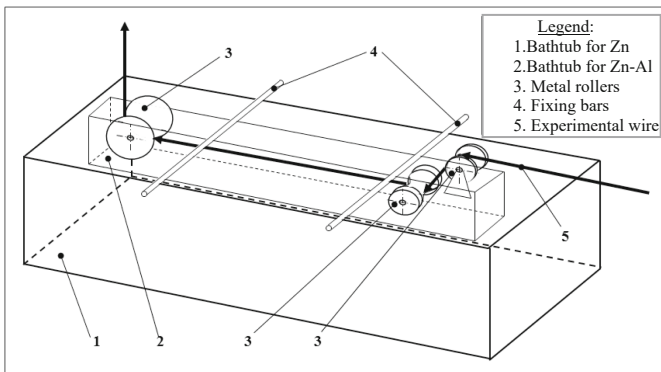


Fig. 1. Sketch of the Zn-Al alloy deposition bathtub.

The temperature range used was from 430 °C to 450 °C and the removal speed (wiping speed) of the steel wire from the bath with molten Zn-Al alloy is identical to that of regular galvanizing. The temperature of the contents of the test bathtub must be extremely precisely known since being semi-submerged (partially submerged) in the galvanizing bathtub, the steel wire adopts the temperature of the outer melt. The fixed

part of the test bathtub was made of ARMCO iron sheet with a thickness of 4.0 mm and the movable part (rollers) with a low carbon content steel.

A second drawing sequence of the protected steel wire was performed starting from an intermediate diameter of 2.0 mm to a final diameter of 1.1 mm, working in a dry version and using dies whose deformation angle 2α was 14° and applying partial reductions of 20%. The drawing series used was: $\varnothing 2.0 \text{ mm} \rightarrow \varnothing 1.8 \text{ mm} \rightarrow \varnothing 1.6 \text{ mm} \rightarrow \varnothing 1.42 \text{ mm} \rightarrow \varnothing 1.26 \text{ mm} \rightarrow \varnothing 1.1 \text{ mm}$ [1].

2 The Chemical Composition of the Protective Layer Deduction Pressing

2.1 Analysis of the Zn-Al Equilibrium Diagram

It has been assumed that the cause lies precisely in the crystallization of the Zn-Al protective layer. The crystallization mode is determined by the chemical composition [2]. In deducing the exact chemical composition, we started from the analysis of the Zn-Al equilibrium diagram that is shown in the Fig. 2.

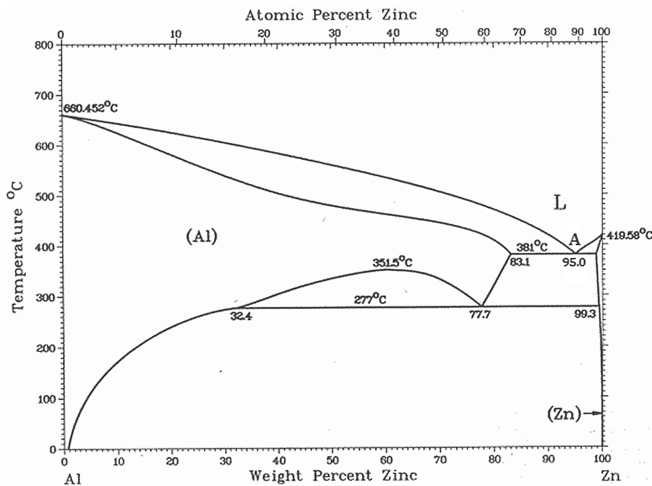


Fig. 2. Zn-Al equilibrium diagram

The really interesting fact in this diagram, from the point of view of the anticorrosive protection of the steel wire but also of the wire drawing manufacturer of that type of wire, is the eutectic, whose chemical composition was 95% Zn and 5% Al. Being Zn in the majority, it is obvious that the structure of the whole resulting ensemble is in hexagonal system. In the case of deformation of the steel wire by wire drawing, when the wire is protected against corrosion in this way, it was observed the almost or total scraping of the protective layer of Zn-Al alloy caused by the pressure and friction inherent to its passage through the die.

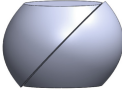
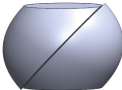



2.2 Pressing Process

It has been considered that the cause of such problems in the wiredrawing process behavior lies precisely in the crystallization way of this protective layer of Zn-Al. For the purpose of this study, different samples with various chemical compositions were prepared, somewhat adjacent to the eutectic A (see Fig. 2), but which no longer crystallized in a hexagonal system. It was considered that, to determine the behavior of the specimens in which the percentage of Zn and Al (initially 95% Zn and 5% Al according to the eutectic A) varied slightly in the vicinity of the initial point A, it is sufficient to evaluate the behavior of a sample of this material when it has undergone compression processing. The following samples of Zn-Al alloy were therefore realized: sample 1–96% Zn and 4% Al, sample 2–95.5% Zn and 4.5% Al, sample 3–95.0% Zn and 5.0% Al, sample 4–94.5% Zn and 5.5% Al and sample 5–94% Zn and 6% Al [3]. We underline the following:

1. Firstly, cylindrical samples were made (their diameter being 10 mm and their height 10 mm).
2. The pressing force was identical for all experiments.

All samples were obtained through casting from liquid (from melted alloy) in metal casting molds.

Table 1. Appearance and chemical composition of the tested samples.

Sample number	The appearance of the cylindrical sample after its pressing	The chemical composition of the sample
1.		96%Zn+4%Al
2.		95.5%Zn+4.5%Al
3.		95.0%Zn+5.0%Al
4.		94.5%Zn+5.5%Al
5.		94.0%Zn+6.0%Al

After solidification the samples were processed on a mechanical press, which performed the pressing at a speed of 0.1 m/s.

The behavior resulting from their pressing process are specified in Table 1.

For the documentation of the presumption of the crystallographic structure and for the demonstration of the new variant of crystallization, the diffractograms of pure Zn and Zn-Al were made (see Fig. 3 and Fig. 4) respectively.

2.3 Resulting Diffractograms

The diffractogram of pure Zn is shown in the Fig. 3 and can be compared with the diffractogram of the Zn-Al alloy with 94.0% Zn and 6.0% Al (Fig. 4):

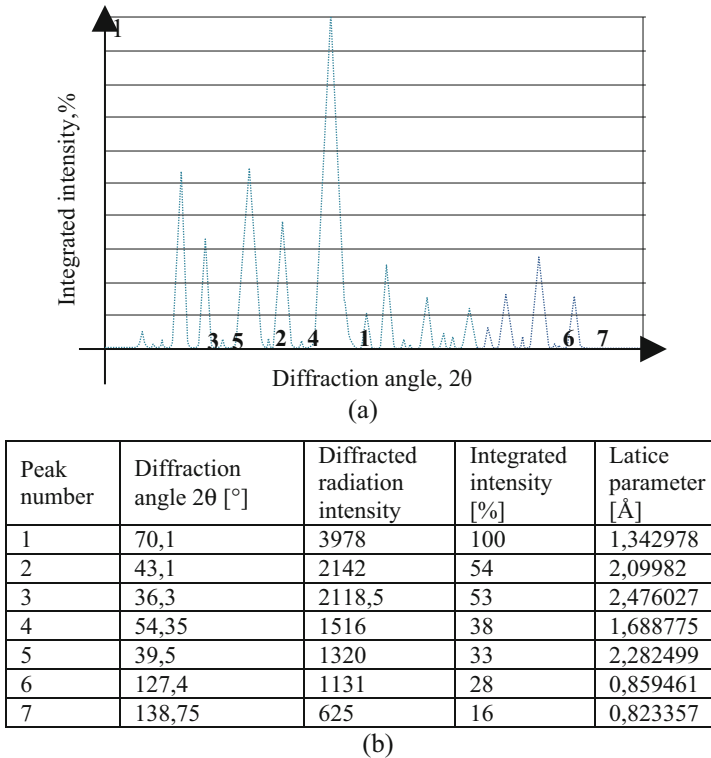
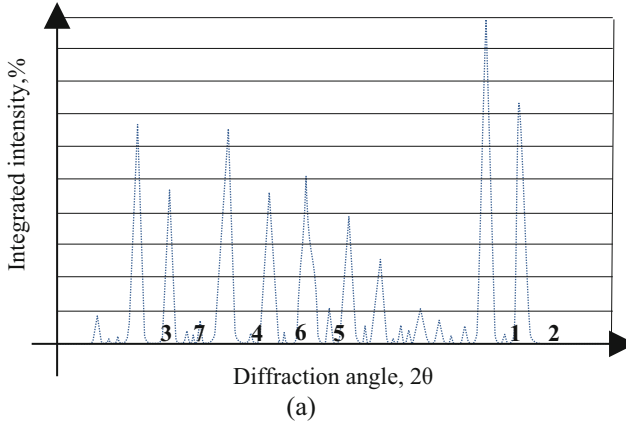


Fig. 3. a) The pure Zn diffractogram; b) explanations of the pure Zn diffractogram.

The arrangement of the peaks “betrays” the adoption for the Zn-Al alloy, in a different crystallization manner than that of pure Zn, which is obviously different in terms of the behavior of the two variants of anticorrosive protection processed by wire drawing. Analyzing the diffractograms of the two crystallization ways, the highlighted characteristics lead to the conclusion of a hexagonal crystallization system, for the case of pure Zn, in contradiction with the cubic crystallization system shown by the Zn-Al alloy.



Peak number	Diffraction angle 2θ [°]	Diffacted radiation intensity	Integrated intensity [%]	Latice parameter [Å]
1	127,2	3980	100	0,860205
2	138,7	2865,8	72	0,812568
3	36	2666	67	2,49597
4	43	2626,8	66	2,104472
5	70	2030	51	1,344651
6	64,1	1870,6	47	1,695987
7	38,75	1831	46	2,324932

(b)

Fig. 4. a)- Zn-Al alloy diffractogram; b)- explanations of the Zn-Al alloy diffractogram.

3 Aluminum Distribution in the Zn-Al Alloy Layer, Deposited on the Surface of a Steel Wire

Following with chemical measurements of the thickness of the deposited layers, an average of 85 μm was obtained for the case of pure Zn coating and about 40 μm for the protective coating with Zn-Al alloy.

Also, photomicrographs of the protective layer of both protective variants were made on the \varnothing 2.00 mm steel wire [4]. The area visualized in the photomicrographs is shown in the Fig. 5 and it was made by embedding the samples in epoxy resin and allowed visualize a portion of the cross section of the steel wire, after applying the specified protective variant. The preparation of the samples and the visual results are shown in the Figs. 5, 6, 7 and 8

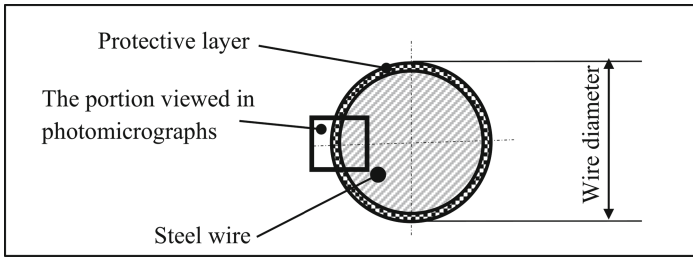
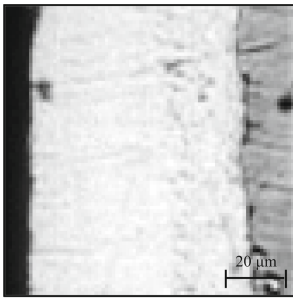
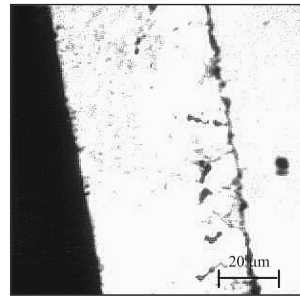


Fig. 5. The cross-sectional portion of the protective coated steel wire, viewed in photomicrographs.

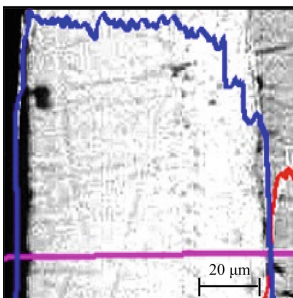


(a)

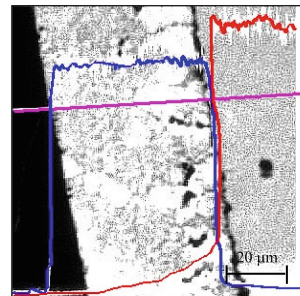


(b)

Fig. 6. Appearance of the protective layer of pure Zn (at a magnification of 2500X): a) respectively Zn-Al alloy; b) deposited on the surface of a steel wire



(a)



(b)

Fig. 7. The compositional profile of Zn (blue) and Fe (red), respectively, on the analysis line (magenta) passing through the deposited protective layer and on a steel wire with a) Zn pure, b) alloy Zn-Al

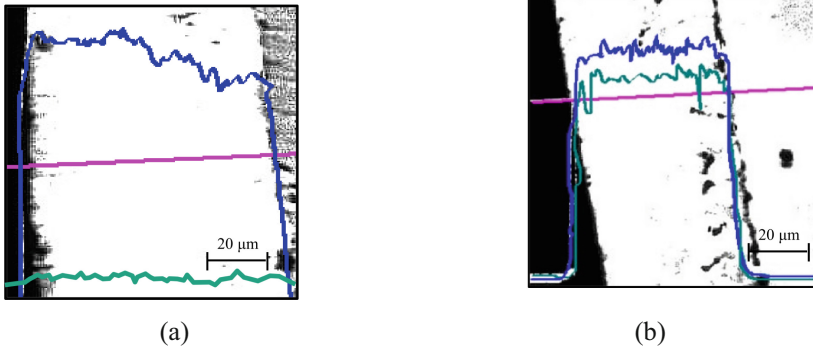


Fig. 8. The compositional profile of Zn (blue) and Al (green), respectively, on the analysis line (magenta) passing through the deposited protective layer and on a steel wire with a) Zn pure, b) alloy Zn-Al [5, 6]

4 Anticorrosive Resistance

The anticorrosive resistance was determined in an Erichsen salt fog installation at the Università degli Studi di Trento, Facoltà di Ingegneria dei Materiali. The duration was monitored as follows: 1. the appearance of “red rust”, 2. the extension of “red rust”, 3. the generalization of “red rust” for hours [7]. The results are specified in the Table 2.

Table 2. Exposure times [in hours] until a certain corrosion stage has been recorded

Type of corrosion protection	Test wire diameter [mm]	Duration until “red rust” appears	Duration until the extension of “red rust”	Duration until the generalization of “red rust”
pure Zn [protection variant 1]	2.0	216	336	432
	1.8	192	216	336
	1.6	168	192	216
	1.42	144	168	192
	1.26	72	144	168
	1.1	72	120	144
Zn-Al alloy (94.0% Zn and 6.0% Al) [protection variant 2]	2.0	336	432	–
	1.8	336	408	–
	1.6	216	336	–
	1.42	216	336	432
	1.26	192	216	336
	1.1	168	192	216

Transposed to graphs, the data deduced for corrosion are shown in the Fig. 9:

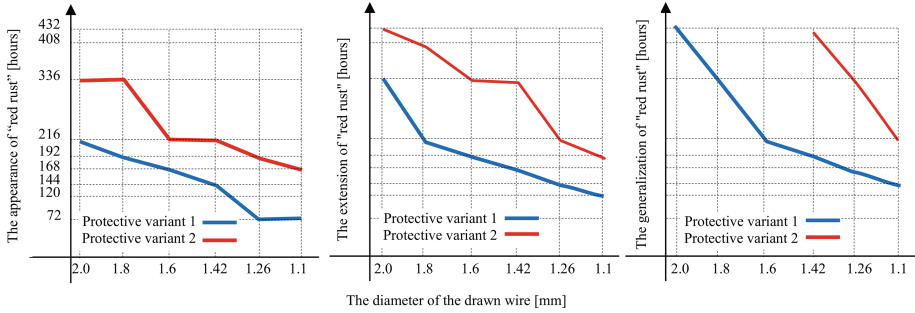


Fig. 9. The stage of corrosion of the steel wire surface during its wire drawing process

5 Conclusions

It has been proven that was adopted the cubic character of the crystallization system of protective variant 2 (with Zn-Al alloy having 94.0% Zn and 6.0% Al) compared to the hexagonal crystallization system adopted by the variant 1 (pure Zn) through diffractograms and pressing behavior [8, 9].

The distribution of Zn and Al were observed both in protective variant 2 (with Zn-Al alloy) and in variant 1 (with pure Zn) in the protective layer deposited on the surface of a steel wire with \varnothing 2.0 mm.

The steel wires protected in one of the specified variants were drawn with the drawing series \varnothing 2.0 mm \rightarrow \varnothing 1.8 mm \rightarrow \varnothing 1.6 mm \rightarrow \varnothing 1.42 mm \rightarrow \varnothing 1.26 mm \rightarrow \varnothing 1.1 mm and the corrosion was controlled (according to the German standard ASTM 117) in an Erichsen salt fog installation at the Università degli Studi di Trento, Facoltà di Ingegneria dei Materiali. It was quantified based on observations made after drawing process and corrosion, considering three different time periods in which certain different stages of corrosion were visible. The recorded time periods (in hours) corresponded to: stage I: appearance of "red rust", stage II: extension of "red rust" and stage III: generalization of "red rust". These recorded durations for each specified diameter practically denoted two things:

- The corrosion duration regresses during both the drawing process, in both protective variants. Regardless of the diameter of the steel wire, the protective variant 2 (with Zn-Al alloy) is always much superior to the protective variant 1 (with pure Zn) [10] (see Table 2)
- Protective variant 2 (with Zn-Al alloy) also proves to be better than protective variant 1, even at a diameter of the steel wire not still deformed by drawing (see the values corresponding to the wire of 2.0 mm in the Table 2)

So, for steel wires either undeformed nor drawn (in a specified technical version), the protective variant 2 (with Zn-Al alloy) confers a corrosion protection clearly superior to the protective variant 1 (with pure Zn) [11].

In the future work, authors will study adhesion of the coating to the steel, processability, and its formability.

References

1. Wright, N.R.: *Wire Technology. Process Engineering and Metallurgy*, Elsevier, ISBN: 978-0-12-382092-1 (2011)
2. Pop, M.: *Plastic Deformations*. ISBN: 978-606-543-509-4 (2014)
3. Yexin, J., Guangling, L.: Development and application of Zn-5% Al-RE alloy coated steel wire. In: *Steel Wire Products* (2001)
4. Pandis, K.P., Papaioannou, S., Siaperas, V., Terzopoulos, A., Stathopoulos, V.N.: Evaluation of Zn- and Fe- rich organic coatings for corrosion protection and condensation performance on waste heat recovery surfaces. *Int. J. Thermofluids* **3–4**, 100025 (2020)
5. Wei, W.A.N.G., Zhi, L.I., Shen, W.J., Yin, F.C., Ya, L.I.U.: Phase equilibria of Zn-Al-Ti ternary system at 450 and 600 °C. In: *Transactions of Nonferrous Metals Society of China*, vol. 30, no. 4, pp. 1005–1016 (2020)
6. Lervik, A., et al.: Atomic structure of solute clusters in Al-Zn-Mg alloys. In: *Science Direct Acta Materialia*, vol. 205, Elsevier (2021)
7. Zhang, L., Ma, A., Jiang, J., Song, D., Chen, J., Yang, D.: Anti-corrosion performance of waterborne Zn-rich coating with modified silicon-based vehicle and lamellar Zn (Al) pigments. *Prog. Nat. Sci. Mater. Int.* **22**(4), 326–333 (2012)
8. Zhang, Z., Yua, J., He, D.: Effect of contact solid solution treatment on peak aging of Al-Zn-Mg-Cu alloys. *J. Mater. Res. Technol.* **9**(3), 6940–6943 (2020)
9. Zha, Z., Tang, J., Haq Tariq, N., Wang, J., Cui, X., Xiong, T.: Microstructure and corrosion behavior of cold-sprayed Zn-Al composite coating. *Coatings* **10**(10), 931 (2020)
10. Tailor, S., Modi, A., Modi, S.C.: Synthesis, microstructural, corrosion and antimicrobial properties of Zn and Zn-Al coatings. *Surf. Eng.* **35**(8), 736–742 (2019)
11. Sugimaru, S., Tanaka, S., Hikita, N., Ohba, H., Yoshie, A., Nishida, S.: Zinc alloy coated steel wire with high corrosion resistance. In: *Nippon Steel Technical Report*, no. 96, pp. 34–38 (2007)